RESEARCH OF A CONTACT STRESSES IN SWIVEL ELEMENTS OF FLEXIBLE SHAFT IN SCREW CONVEYOR FOR TRANSPORTATION OF AGRICULTURAL MATERIALS

Volodymyr Bulgakov[1], Jüri Olt[2], Semjons Ivanovs[3], Oleksandra Trokhaniak[1], Jaroslav Gadzalo[4], Valerii Adamchuk[5], Mykhailo Chernovol[6], Simone Pascuzzi[7], Francesco Santoro[7], Margus Arak[2]

[1]*National University of Life and Environmental Sciences of Ukraine, 15 Heroiv Oborony St., UA 03041 Kyiv, Ukraine*
[2]*Estonian University of Life Sciences, Institute of Forestry and Engineering, 56 Kreutzwaldi St., 51006 Tartu, Estonia*
[3]*Latvia University of Life Sciences and Technologies, 5 Cakstes Blvd., LV 3001 Jelgava, Latvia*
[4]*National Academy of Agrarian Sciences of Ukraine, 9, Mykhailo Omelyanovych-Pavlenko St., UA 01010, Kyiv, Ukraine*
[5]*Institute of Mechanics and Automation of Agricultural Production of the National Academy of Agrarian Sciences of Ukraine, 11 Vokzalna St., Glevakha Stl., Vasylkivsky Dist., UA 08631, Kyiv Region, Ukraine*
[6]*Central Ukrainian National Technical University, University Ave., 8, UA 25006 Kropivnitskyi, Kirovograd region, Ukraine*
[7]*University of Bari Aldo Moro, Department of Agricultural and Environmental Science,*
Via Amendola 11 165/A, 70126 Bari, Italy

ABSTRACT. The paper presents the new design of the rotating part with ball-bearing swivel joints between its sections for flexible screw conveyors. The new design provides for the improvement of the operation efficiency and loading capacity, the enhancement of the technological capabilities and the reduction of the admissible curvature radius. The contact stresses in the swivel element as the most loaded area in the rotating part have been analysed. It has been established that the maximum contact stresses arise at the points of contact between the ball and the flat surface of the slot in the cylindrical bushing. The recommended design limitation range for the cavity cone angle is within about 30–50°. The relation between the loads and the stresses depending on the operating conditions has been modelled with the use of computer modelling. The comparison of the computer modelling results and the obtained calculation data has proved that the difference between the respective values varies within the range of 11–26%.

Introduction

The equipment for continuous transportation of agricultural materials is the basis for the comprehensive mechanisation of the loading/unloading operations that are implemented to raise the productivity of labour and the efficiency of production (Lech, 2001; Gill, 2003; Loveikin, Rogatynska, 2011; Evstratov *et al.*, 2015; Lyashuk *et al.*, 2015; Olanrewaju *et al.*, 2017; Karpeenko *et al.*, 2021). In agricultural and industrial production, there exists a whole range of machinery for

the loading and discharge of bulk materials (grain crops, compound animal feedstuff, mineral fertilisers, sand, commercial salt, shredded metal chips etc.).

The completed review has resulted in a conclusion that, in the case of curvilinear transportation routes, flexible screw conveyors, the rotating part of which is designed as several individual screw sections connected with swivel joints, represent the least resource-intensive technology for bulk material transportation (Frey *et al.*, 2012; Hevko *et al.*, 2016, 2017, 2018a; Trokhaniak *et al.*, 2020). However, the existing flexible screw conveyors do not fully meet the operation requirements applied to such types of conveyors. For example, the use of continuous helical spirals as flexible augers results in their rapid failure due to the action of alternating cyclic loads (Olanrewaju *et al.*, 2017; Baranovsky *et al.*, 2020; Evstratov *et al.*, 2020; Hevko *et al.*, 2018b and 2020).

Sectioned augers feature structural complexity, complicated production techniques and high material intensity, as regards their production. In operation, they have increased power consumption (Tian *et al.*, 2018; Hevko *et al.*, 2021) and damage the transported material and the internal surfaces of the flexible pipes (Rohatynskyi *et al.*, 2016; Manjula *et al.*, 2017; Hevko *et al.*, 2019). Hence, developing new designs of the flexible screw-type operating parts in auger conveyors

and analysing the selection of their parameters to improve the operating efficiency of such conveyors is a task of current concern.

The purpose of the work was theoretical research and calculation definition of contact stresses in swivel elements of a flexible shaft in a screw conveyor.

Materials and Methods

To increase the operating efficiency and throughput of flexible screw conveyors and enhance their process capacities, the authors have developed various designs of sectioned augers with ball swivel joints between the sections.

The sectioned operating part of the screw conveyor is designed as the identical spirals 1 and 2, each made from a flat bar with a thickness of δ and supported by n section core rods (Fig. 1). The ends of the spirals are rigidly attached by their inside edges to the left split-design bushing 3 and the right splined bushing 4, respectively. The said bushings are rigidly connected via the rotation spring coil 5. Inside the spring coil, the swivel bolt joint passes. The bolt shank 6 is splined and its free right end is inserted into the right internally splined bushing so that the splines of the bolt and the bushing interact with each other.
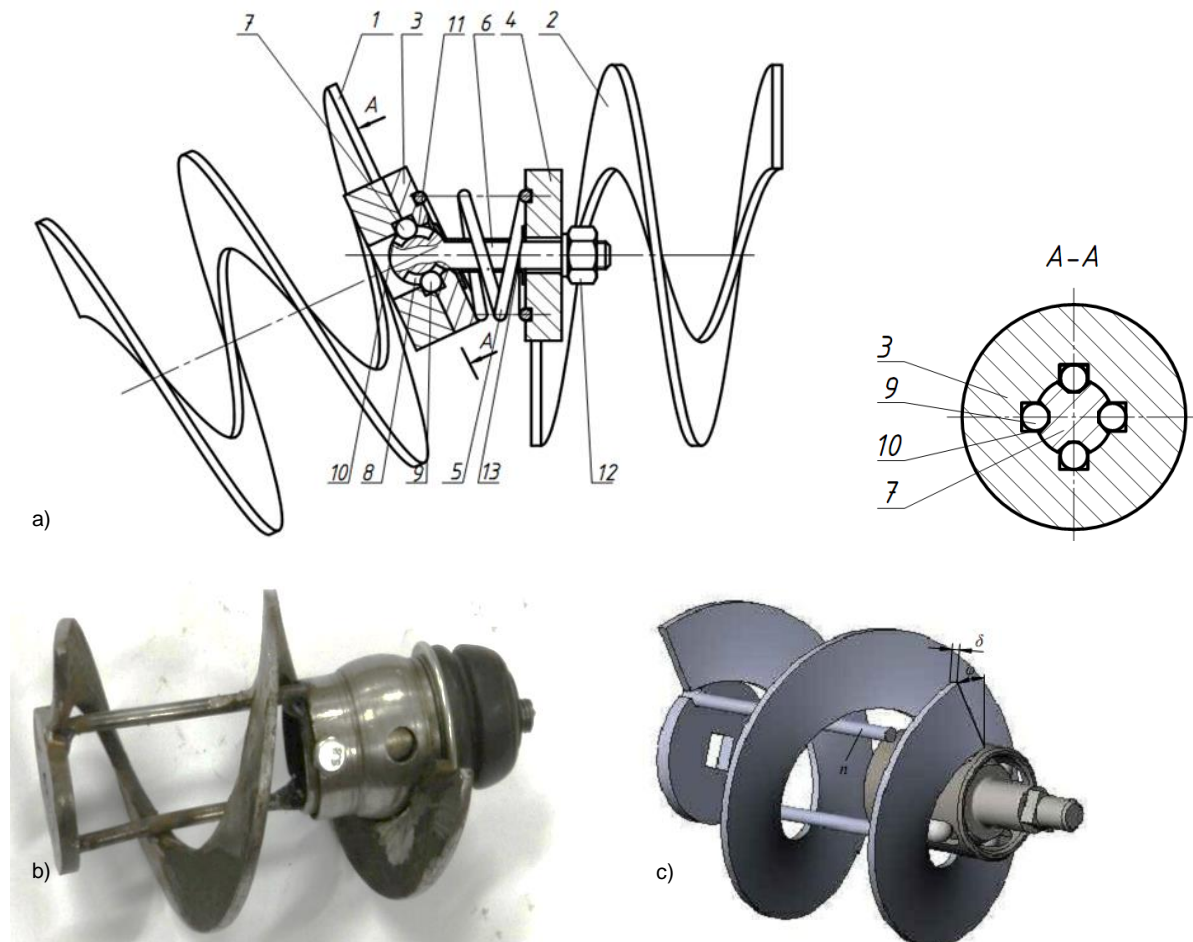

Figure 1. Structural layout (a), general view (b) and 3-D model (c) of auger section for screw conveyor

The left end of bolt 6 is made in the form of the spherical head 7, on the surface of which four equally spaced races with semi-circular cross-sections are symmetrically positioned on the respective great circles. The races interact with the balls 9, which are freely placed in the internal spherical cavities 10 of the left bushing 3. The spherical surface 7 of bolt 6 interacts with the semi-spherical aperture 11 of bushing 3. The latter is assembled from its two halves, which are rigidly connected with the use of standard methods and provide for the free rotation of the head 7 of the bolt 6. Thus, bolt head 7 in the bushing 3 acts as a universal joint. The two screw sections 1 and 2 are connected by the bolt joint with the nut 12. To seal the bolt connection, the shank of bolt 6 is covered with the elastic jacket 13, which prevents the bulk material from entering the friction zone.

In Figures 1b and 1c, the general view and 3-D model of the screw auger section, respectively, are shown. The sectioned auger operates as follows. When one helical spiral section rotates, the rotary motion is imparted by the spiral 1 to the left split-design bushing 3, the ball 9, the spherical bolt head 7, the splined bolt shank 6, the right splined bushing 4 and finally to the spiral 2. An additional rotary motion transmission path is the spring 5, which is rigidly attached by its ends to the left 3 and right 4 bushings.

To determine the contact stresses, the analysis has been carried out for the most strained element in the swivel joint auger, which is the ball that has a contact at three points with different surfaces in the joint and transfers the main torque T (Fig. 2). As the swivel joint, the two axes of which are displaced by a certain angle rotates, the ball moves on the surface of the casing and the surface of the race. This motion involves sliding, which implies the rise of friction forces. These forces depend on many factors. Each friction force is aligned with the respective instantaneous line of travel of the ball and is at a right angle to the line of action of the respective pressure force. The three friction forces F_{f1}, F_{f2} and F_{f3} are shown in Figure 2. Their lines of action change in the course of the ball rotation.
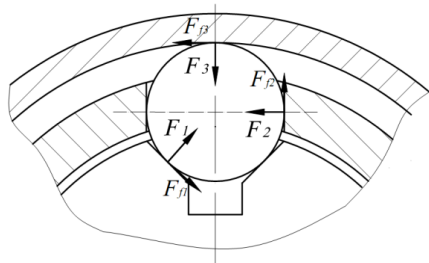

Figure 2. Analytical model for determining parameters of forces acting on the ball, when it transfers torque

The ball is under the action of the three forces F_1, F_2 and F_3 applied to it by the conical cavity, the slot in the cylindrical bushing and the spherical part of the casing, respectively. Each of the forces generates significant contact stresses. The stresses have to be analysed to determine the design parameters and limits that ensure the integrity and operating capacity of the swivel joint structure. At all three points of contact, the types of contact surfaces are different. The force F_1 acts in the area of contact between the ball and the conical surface of the race. This contact can be analysed as the contact between the spherical surface and the equivalent cylindrical surface. The contact in the area of action of the force F_2 is between the spherical surface of the ball and the plane.

The last of the three points, where the force F_3 is transferred, features an inside spherical contact. As is obvious from the above, the contact surfaces in the three cases under consideration are different. Therefore, it is necessary to analyse and calculate them individually. In the case of the contact between two spheres (the contact between the ball and the spherical surface of the bushing), the curvatures in the principal planes of the bodies have the following values:

$$k_{11} = k_{12} = \frac{1}{r} \cdot \tag{1}$$

$$k_{21} = k_{22} = \frac{1}{R+r}, \tag{2}$$

where r – radius of the ball, $R+r$ – radius of the spherical surface of the bushing.

As the spherical contact is an inside contact, the radius of the greater sphere has to be assumed with the minus sign, therefore, the respective coefficients appear as follows:

$$A = B = \frac{1}{2}\left(\frac{1}{r} - \frac{1}{R+r}\right) = \frac{R}{2r(R+r)}, \tag{3}$$

where A is the mean curvature:

$$\sum k = 2(A+B) = \frac{2R}{r(R+r)} \cdot \tag{4}$$

The contact patch for a force of F is a circle with the following radius:

$$a = \sqrt[3]{\frac{3\eta F}{2\sum k}}, \tag{5}$$

where

$$\eta = 2\frac{1-v^2}{E} \cdot \tag{6}$$

E and v – Young's modulus of elasticity and Poisson's ratio, respectively, for the material of the ball and the swivel joint (they are assumed both to be made of steel).

The maximum pressure on the contact patch surface:

$$p_0 = \frac{1}{\pi}\sqrt[3]{\frac{3F(\sum k)^2}{2\eta^2}} \cdot \tag{7}$$

The mean pressure within the contact patch:

$$p = \frac{2}{3} p_0 . \qquad (8)$$

After substituting the expressions for all the coefficients, the following final formula is obtained for the calculation of the maximum pressure at the contact between the ball and the spherical surface of the bushing:

$$p_{03} = \frac{1}{\pi} \sqrt[3]{\frac{3F_3 R^2 E^2}{2r^2 (R+r)^2 (1-v^2)^2}} . \qquad (9)$$

The calculation of the contact stresses at the contact between the ball and the plane is of a similar type, but the values of the coefficients and the curvature are determined assuming that the radius of the plane is equal to infinity (its curvature is equal to zero). Thus:

$$A = B = \frac{1}{2r} ; \qquad (10)$$

$$\sum k = 2(A+B) = \frac{2}{r} . \qquad (11)$$

After appropriate transformations, the maximum pressure at the contact between the ball and the flat surface of the slot in the cylindrical bushing is represented by the following relation:

$$p_{02} = \frac{1}{\pi} \sqrt[3]{\frac{3F_2 E^2}{2r^2 (1-v^2)^2}} . \qquad (12)$$

The task of calculating the pressure at the contact between the ball and the conical cavity is somewhat more complex. Since the pressure force F_1 acts at a right angle to the generatrix of the cone, it is necessary to assume the interacting contact surfaces as a spherical one (the ball) and a cylindrical one (the cone), with a mean radius at the point of contact. The mean radius of the equivalent cylinder at the point of contact has to be equal to the radius of the line produced by the intersection of the cone with the perpendicular plane.

According to Rogatynska *et al.*, (2015):

$$K' = \frac{K}{\cos \gamma} , \qquad (13)$$

where K and K' – the curvature of the conic section that is at a right angle to the axis of the cylinder and the curvature of the conic section that is at an angle γ to this plane, respectively.

Angle γ is the cone apex angle, that is, the angle between the perpendicular to the cone generatrix and the cone base plane. The cone base radius R_k at the contact between the ball and the cavity determines the curvature K' and, taking into account the geometrical considerations, they are calculated by the following formulae:

$$R_k = r \cos \gamma ; \qquad (14)$$

$$K' = \frac{1}{r \cos \gamma} . \qquad (15)$$

Hence, the curvature of the equivalent cylinder is equal to:

$$K = \frac{1}{r} , \qquad (16)$$

while its radius is equal to:

$$R_c = r . \qquad (17)$$

The radius of the equivalent cylinder is identical to the radius of the ball, which significantly reduces the contact stress at the internal contact.

Using the formula (Grote, Feldhusen, 2007), the following is obtained:

$$A = \frac{1}{2r} ; \qquad (18)$$

$$B = 0. \qquad (19)$$

Accordingly, the sum of curvatures is equal to:

$$\sum k = 2(A+B) = \frac{1}{r} . \qquad (20)$$

After substituting the above-mentioned coefficients into the expression for the calculation of contact stresses and applying the respective tabulated reference data, the following formula is obtained for the calculation of the contact stresses at the surface of the cavity:

$$p_{01} = \frac{0.4}{\pi} \sqrt[3]{\frac{3F_1 E^2}{8r^2 (1-v^2)^2}} . \qquad (21)$$

The values of the forces applied at the points of contact can be expressed in terms of the torque T:

$$F_1 \cdot \cos \gamma = F_2 ; \qquad (22)$$

$$F_1 \cdot \sin \gamma = F_3 ; \qquad (23)$$

$$F_2 = T \cdot (NR \cdot \cos \alpha)^{-1} , \qquad (24)$$

where α – angular displacement of the bolt with a spherical head; N – number of the balls in the joint.

Finally, the following formulae are obtained for the calculation of the contact stresses:

$$p_{01} = \frac{0.4}{\pi} \sqrt[3]{\frac{3TE^2}{8NRr^2 (1-v^2)^2 \cos \alpha \cos \gamma}} . \qquad (25)$$

$$p_{02} = \frac{1}{\pi} \sqrt[3]{\frac{3TE^2}{2NRr^2 (1-v^2)^2 \cos \alpha}} . \qquad (26)$$

$$p_{03} = \frac{1}{\pi} \sqrt[3]{\frac{3TRE^2 \mathrm{tg}\gamma}{2Nr^2 (R+r)^2 (1-v^2)^2 \cos \alpha}} . \qquad (27)$$

Thus, the formulae have been obtained for the calculation of the contact stresses in the most loaded element, which is the ball that has a contact at its three

points with different surfaces of the structure and takes part in the transfer of the main torque T.

It has been established by the authors that various methods can be used to select such geometric parameters of the swivel joint that ensure, under the given contact forces and with the use of adequate materials, the conditions, in which the maximum stresses do not exceed the permissible ones.

Results and Discussion

Using the results of the PC-assisted calculations carried out based on the system of equations (25–27) and assuming that $R = 17$ mm, $r = 4.75$ mm, $N = 4$ and $E = 2 \cdot 10^{11}$ N m^{-2}, $v = 0.25$, the graphic relations between the contact stresses and the cavity cone angle γ, the angular displacement of the spherical head bolt α and the torque T have been plotted, as shown in Figure 3.
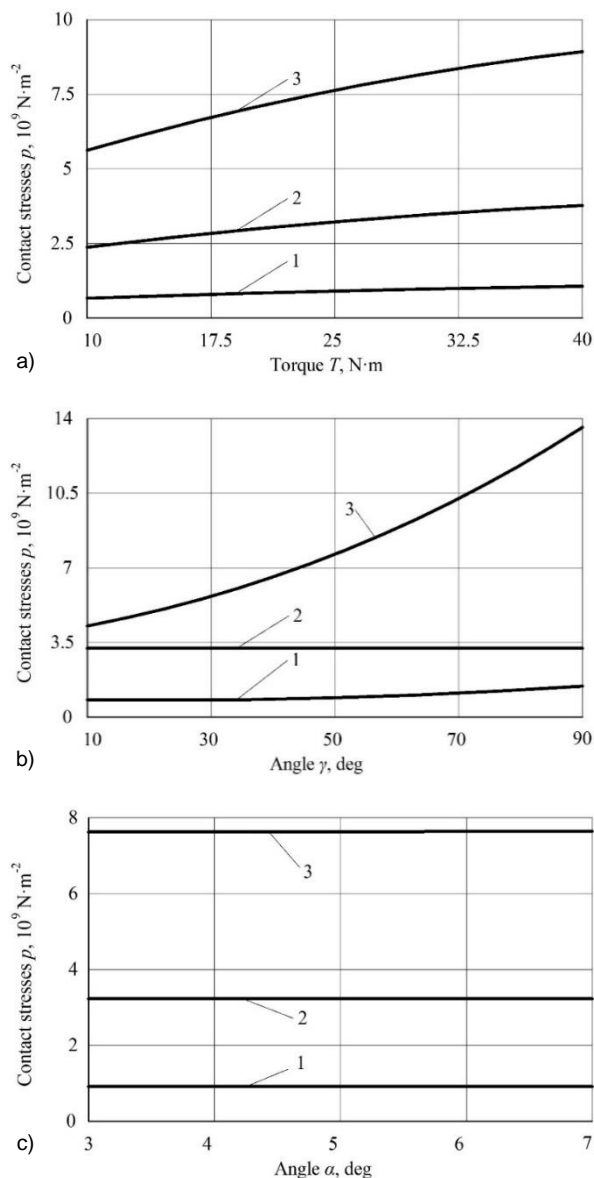

Figure 3. Graphic relations between contact stresses p and torque T (a), cavity cone angle γ (b) and angular displacement of spherical head bolt α (c): $1 - p_{02}$; $2 - p_{02}$; $3 - p_{03}$

The analysis of the obtained diagrams (Fig. 3) and equations (25–27) has proved that, when the parameters of the joint are selected correctly, the maximum contact stresses arise at the point of contact between the ball and the flat surface of the slot in the cylindrical bushing. They can be calculated with the use of the formula for p_{02}. The recommended structural limitation range for the cavity cone angle is approximately 30–50 degrees. When these limits are exceeded, the stresses in other elements of the swivel joint sharply rise. The main element in the transfer of the torque is the contact at the flat surface of the slot in the cylindrical bushing. The rather small values of the contact stresses that arise in the cavity can be explained by the large contact patch area extending along almost the whole ball seating line.

It has been established that the maximum effect on the magnitude of the contact stresses p arising in the elements of the swivelling-section auger is produced by the torque T (Fig. 3a, its variation within the range of 10–40 Nm results in the stresses p increasing by 35–37%). The other factors that affect the magnitude of the contact stresses are the cavity cone surface generatrix angle γ (Fig. 3b, when γ increases from 30 to 50°, the stresses rise by 9–21%) and the angular displacement α of the spherical head bolt (Fig. 3c, when α varies from 3 to 7°, the stresses increase by 0.3%).

To find the optimum design characteristics of the screw auger sections, computer simulation has been carried out to determine the contact stresses in auger components concerning the operating conditions.

Within the Solid Works application environment, a computer model has been generated for an auger section in the flexible screw conveyor complete with the swivel-joint transmission devices attached to the section. The general view of the model with the applied load is shown in Figure 4. One intermediate element is rigidly fixed (shown on the left in Fig. 4), and the torque is applied to the other one (as shown on the right).
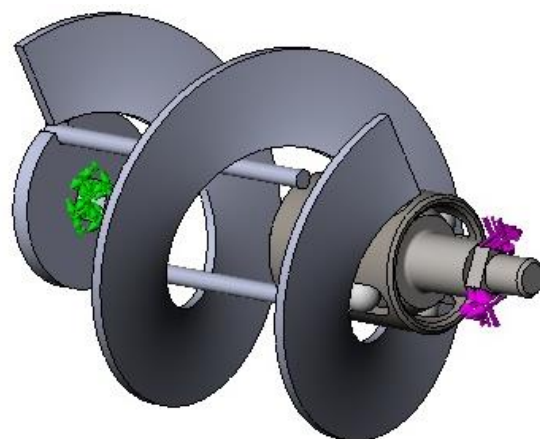

Figure 4. Model of a section with load applied to it

Because of the modelling process, the following graphic representation of the stresses that arise in the auger components under the action of the applied torque (Fig. 5) has been displayed in the application window.
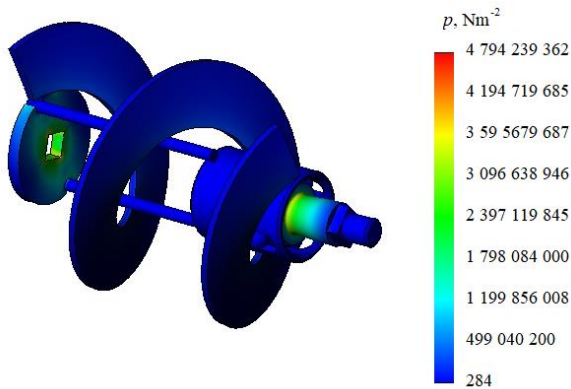
Figure 5. Diagram of stresses in components of auger section

The analysis of the obtained results has proved the agreement of the obtained values and the respective graphic relations plotted on their basis. The comparison of the computer modelling results and the data obtained using calculation has shown that the difference between the corresponding values varies within the range of 11–26%.

Conclusion

It has been established that the maximum contact stresses arise at the points of contact between the ball and the flat surfaces of the slot in the cylindrical bushing. The recommended range of structural limitation for the cavity cone angle lies within about 30–50 degrees.

It has been proved that the maximum effect on the magnitude of the contact stresses p generated in the components of the swivel-joint sectioned auger is produced by the torque T (when it varies within the range of 10–40 Nm, the stresses p increase by 35–37%). At the same time, the magnitude of the contact stresses also depends on the cavity cone surface generatrix angle γ (if γ is increased from 30 to 50°, the stresses rise by 9–21%) and on the angular displacement of the spherical head bolt α (when α changes from 3 to 7°, they increase by 0.3%).

Conflict of interest

The authors declare that they have no known competing financial interests or personal relationships that could have appeared to influence the work reported in this paper.

Author contributions

VB, JO, OT – study conception and design;
VB, JO – drafting of the manuscript;
VB, VA, JO, MA, OT – analysis and interpretation of data;
JG, MA, MC, SI, SP, FS – acquisition of data.
JO – critical revision and approval of the final manuscript.
All authors have read and agreed to the published version of manuscripts

References

Baranovsky, V., Trahanska, O., Pankiv, M., Bandura, V. 2020. Research of a contact impact of a root crop with a screw auger. – Research in Agricultural Engineering, 66(1): 33–42. DOI: 10.17221/75/2017-RAE

Evstratov, V.A., Linnik, Y.N., Linnik, V.Y., Grigoryev, V.I., Suxarnikova, V.A. 2020. Structural and parametric synthesis of screw modules of technological machines. – IOP Conference Series: Materials Science and Engineering, 843(1):012016. DOI: 10.1088/1757-899X/843/1/012016

Evstratov, V.A., Rud, A.V., Belousov. K.Y. 2015. Process modelling vertical screw transport of bulk material flow. – Procedia Engineering, 129: 397–402. DOI: 10.1016/j.proeng.2015.12.134

Frey, S., Dadalau, A., Verl, A. 2012. Expedient modeling of ball screw feed drives. – Production Engineering, 6 (2): 205–211. DOI: 10.1007/s11740-012-0371-0

Gill, D.R. 2003. Basics of flexible screw conveyors. – Plant Engineering, 57(1):46–48.

Grote, K.-H., Feldhusen, J. 2007. Dubbel: Taschenbuch für den Maschinenbau. – Springer, Deutchland, 1798 pp.

Hevko, B.M., Hevko, R.B., Klendii, O.M., Buriak, M.V., Dzyadykevych, Y.V., Rozum, R.I. 2018a. Improvement of machine safety devices. – Acta Polytechnica, Journal of Advanced Engineering, 58(1):17–25. DOI: 10.14311/AP.2018.58.0017

Hevko, R.B., Klendiy, M.B., Klendiy, O.M. 2016. Investigation of a transfer branch of a flexible screw conveyer. – INMATEH - Agricultural Engineering, 48(1):29–34.

Hevko, R., Rohatynskyi, R., Hevko, M., Lyashuk, O., Trokhaniak, O. 2020. Investigation of sectional operating elements for conveying agricultural materials. – Research in Agricultural Engineering, 66(1):18–26.

Hevko, R.B., Strishenets, O.M., Lyashuk, O.L., Tkachenko, I.G., Klendii, O.M., Dzyura, V.O. 2018b. Development of a pneumatic screw conveyor design and substantiation of its parameters. – INMATEH - Agricultural Engineering, 54(1):153–160.

Hevko, R., Vitrovyi, A., Klendii, O., Liubezna, I. 2017. Design engineering and substantiation of the parameters of sectional tools of flexible screw conveyers. – Bulletin of the Transilvania University of Brasov, 59(10):39–46.

Hevko, R., Zalutskyi, S., Hladyo, Y., Tkachenko, I., Lyashuk, O., Pavlova, O., Pohrishchuk, B., Trokhaniak, O., Dobizha, N. 2019. Determination of interaction parameters and grain material flow motion on screw conveyor elastic section surface. – INMATEH - Agricultural Engineering. 57(1):123–134.

Hevko, R., Zalutskyi, S., Tkachenko, I., Lyashuk, O., Trokhaniak, O. 2021. Design development and study of an elastic sectional screw operating tool. – Acta Polytechnica. 61(5):624–632. DOI: 10.14311/AP.2021.61.0624

Karpeenko, A., Kuznetsov, Y., Bychkova, T., Kravchenko, I., Aldoshin, N., Kalashnikova, L. 2021. Grain auger conveyor-distributor. – INMATEH - Agricultural Engineering, 65(3):39–46. DOI: 10.35633/INMATEH-65-04.

Lech, M. 2001 Mass flow rate measurement in vertical pneumatic conveying of solid. – Powder Technology, 114(1–3):55–58.

Loveikin, V., Rogatynska, L. 2011. A model of loose material transportation by means of high-speed conveyors with elastic operating devices. – Bulletin of I. Puluj Ternopil National Technical University, 16:66–70.

Lyashuk, O.L., Rogatynska, O.R., Serilko, D.L. 2015. Modeling of the vertical screw conveyer loading. – INMATEH - Agricultural Engineering, 45(1):87–94.

Manjula, E.V.P.J., Hiromi, W.K. Chandana, A.B., Melaaen, M.C. 2017. A review of CFD modelling studies on pneumatic conveying and challenges in modelling offshore drill cuttings transport. – Powder Technology, 305:782–793, DOI: 10.1016/j.powtec.2016.10.026. ISSN 0032-5910.

Olanrewaju, T.O., Jeremiah, I.M., Onyeanula, P.E. 2017. Design and fabrication of a screw conveyor. – Agricultural Engineering International: CIGR Journal, 19(3):156–162.

Rogatynska, O., Liashuk, O., Peleshok, T., Liubachivskyi, R. 2015. Investigation of the process of loose material transportation by means of inclined screw conveyers. – Bulletin of I. Pyliui Ternopil National Technical University, 79:137–143.

Rohatynskyi, R.M., Diachun, A.I., Varian, A.R. 2016, Investigation of kinematics of grain material in a screw conveyor with a rotating casing. – Bulletin of Kharkiv Petro Vasylenko National Technical Univarsity of Agriculture, 168:24–31.

Tian, Y., Yuan, P., Yang, F., Gu, J., Chen, M., Tang, J., Su, Y., Ding, T., Zhang, K., Cheng, Q. 2018. Research on the principle of a new flexible screw conveyor and its power consumption. – Applied Sciences (Switzerland), 8(7):1038. DOI: 10.3390/app8071038

Trokhaniak, O.M., Hevko, R.B., Lyashuk, O.L., Dovbush, T.A., Pohrishchuk, B.V., Dobizha, N.V. 2020. Research of the bulk material movement process in the inactive zone between screw sections. – INMATEH - Agricultural Engineering, 60(1):261–268, DOI: 10.35633/INMATEH-60-29.